Experimental Investigation of Particle Pinch Associated with Turbulence in LHD Heliotron and JT-60U Tokamak Plasmas

K. Tanaka 1), H. Takenaga 2), K. Muraoka 3), C. Michael 4), L. N. Vyacheslavov 5), M. Yokoyama 1), H. Yamada 1), N. Oyama 2), H. Urano 2), Y. Kamada 2), S. Murakami 6), A. Wakasa 7), T. Tokuzawa 1), T. Akiyama 1), K. Kawahata 1), M. Yoshinuma1), K. Ida 1), I. Yamada 1), K. Narihara 1), N. Tamura 1) and the LHD experimental group 1)

1)National Institute for Fusion Science, Toki 509-5292, Japan
2)Japan Atomic Energy Agency, 801-1 Mukouyama, Naka, Ibaraki 311-0193, Japan
3)Chubu University, 1200 Matsumoto, Kasugai, Aichi 487-8501, Japan
4) EURATOM/UAKEA Fusion Association, Oxfordshire OX14 3 DB, United Kingdom
5) Budker Institute of Nuclear Physics, 630090, Novosibirsk, Russia
6) Department of Nuclear Engineering, Kyoto University, Kyoto 606-8501, Japan

e-mail contact of main author: ktanaka@LHD.nifs.ac.jp

Abstract. Comparative studies were carried out to elucidate the most essential parameter(s) for control of density profiles in LHD heliotron and JT-60U tokamak plasmas. Clear differences and similarities of the characteristics of density profiles have been found among both plasmas in the low collisionality regime. Role of turbulence was experimentally investigated in both devices during change of density profiles under scanning neutral beam (NB) heating power. Changes of spectrum structure and power were observed. .

1. Introduction

Understanding of physics mechanism of electron density profiles is one of the essential issues for control of future fusion reactor in both heliotron/stellarator and tokamak devices. Many experimental works and theoretical investigations were done. These suggest role of neoclassical effects and turbulence. The former is due to the collision process of confined particle and the theoretical mode is well developed. The latter is due to effect of the turbulence, which are due to ion temperature gradient mode (ITG) and trapped electron mode (TEM). In the both devices, in the limited operation regime, neoclassical effect can account for experimental observation, however, in many other regime, neoclassical effects is not strong enough to account for observed density profiles. Many theoretical models of anomalous particle transport were proposed, but, none of this cannot explain experimental observations. In addition, experimentally it is not clear if turbulence can play role on density profile because of limited measurements in plasma core region. Therefore, it is essential to study relation between turbulence and density profile for the further understanding.

2. General comparison of density profiles between JT60-U and LHD

Figure 1 shows radial profiles of electron density (n_e) and electron temperature (T_e) of JT-60U and LHD with neutral beam (NB) heating. Clear differences of density profiles can be seen for the different densities in JT-60U and for the different magnetic axis positions (R_{ax}) in LHD. Particle sources from walls decreased exponentially and did not affect the core density profiles (at $\rho<1.0$) in both devices. In JT-60U, the central particle source was changed by a factor three by the combination of NB and electron cyclotron heating powers. However, the density peaking factor did not change [1]. In LHD, central particle fueling was increased by a factor eight with an increase of NB powers at R_{ax}=3.6 m, resulting in the change of density

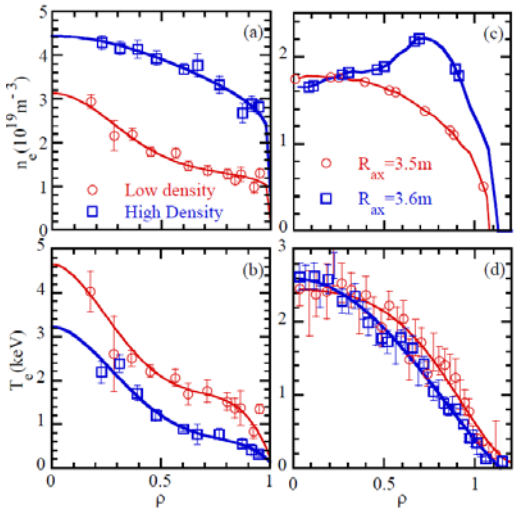

Fig. 1 (a), (c) n_e, and (b),(d) T_e profiles. (a) and (b) from JT-60U, and (c) and (d) from LHD. Here, plasmas in low and high density plasmas in JT-60U, and those at R_{ax}=3.5m and R_{ax}=3.6m in LHD are compared.

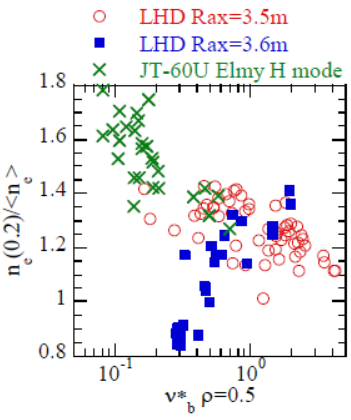

*Fig.2 Dependence of the density peaking factor on ν_b**

profiles from peaked to hollow although NB fueling supplied particles more to the core than to the edge [2]. Carbon impurity profiles did not change in both devices in Fig. 1, indicating that impurity accumulation did not affect density profiles. These observations suggest the changes of density profiles to be not due to the difference of particle fueling, but due to the difference of transport in both devices. In JT-60U, the contribution of the neoclassical Ware pinch was negligible, thus requiring to invoke an anomalous inwardly directed pinch. As shown in Figs. 1 (a) and (b), the density profile in JT-60U is more peaked at a low value of n_e and/or a high value of T_e. This fact may indicate an anomalous inward pinch being larger with decreasing collisionality. In LHD, neoclassical transport was minimized by reducing the effective helical ripple at around R_{ax}=3.5-3.6 m [3]. Neoclassical transport was almost the same amount for both positions of R_{ax}. Therefore, the observed difference of density profiles is due to the contribution of anomalous transport for R_{ax} = 3.5 m and 3.6 m.

Figure 2 shows the dependence of density peaking factors on an electron-ion collision frequency normalized by the trapped electron bounce frequency (ν^*_b). The density peaking factor was defined as the ratio of the density at ρ=0.2 against the volume averaged density and ν^*_b was estimated at ρ=0.5. As shown in Fig. 2, density peaking factors increased with decreasing ν^*_b in JT-60U. The origin of density peaking in tokamaks is theoretically suggested as due to the turbulence-driven inward pinch, resulting in the increase of the density peaking factor with decreasing collisionality [4]. On the other hand, a different ν^*_b dependence was observed at R_{ax}=3.5 m and 3.6 m in LHD. At R_{ax}=3.5 m, density peaking factors moderately increased with decreasing ν^*_b. In addition, only peaked density profiles were observed. Both of these observations are similar characteristics with those for JT-60U, suggesting common underlining physics. On the other hand, for R_{ax}=3.6 m, density peaking factors decreased with decreasing ν^*_b. Particle convection velocities for R_{ax}=3.6 m, which were estimated using a density-modulation experiment [2], were outwardly directed and close to neoclassical values at lower collisionality, suggesting that particle transport (thus the observed ν^*_b dependence shown in Fig. 2) be affected by neoclassical processes.

3. Response of turbulence under change of density profiles in JT-60U

Density profile becomes peaked one at lower collisionality. Thus increase of NB power with constant external fueling induce density peaking. Figure 3 and 4 shows such examples in the

similar Elmy H mode discharge to the data set of Fig.2. NB powers increase from 7.4 to 12.9MW in time as shown in Fig.3. (a), then, density profile became slightly peaked as shown in Fig.3 (a). Central line integrated density increases with increase of NB power as shown in Fig.3 (b), however, the increase of beam source is not dominant effect as described in the previous section.

The characteristic of turbulence was measured by O mode correlation reflectometry [5]. Two close frequency microwave, where one is fixed at 47.3GHz the other is scanned 42.3-46.8GHz in 6 step in time. Each step is 20ms, then cross correlation of the reflected power was measured in 120msec for the density regimes 2.23-2.78x$10^{19}$$m^{-3}$. The coherence was estimated at -500-500kHz and averaged in every 50kHz segments. Highest coherence was selected as a representative values and standard deviation in the each segments was error bar of the coherence in Fig.5. The radial correlation length (l_c) was estimated from radial profile of the coherence like in Fig.5. For the quantitative estimation of l_c, the radial correlation profile was determined from the exponential fitting function, which is coh(δR)=exp(-δR/l_c).

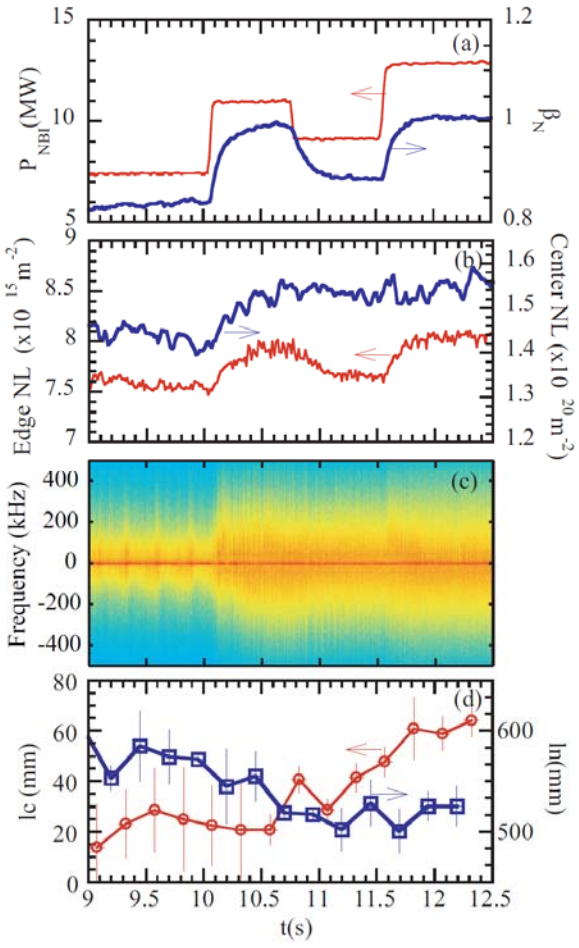

Fig.3 Time history of (a) NB power, nolmalized beta (β_n), (b) line integrated density (c)reflected power spectrum and (d)density scale length,

Figure 3 (c) shows time history of power spectrum of fixed frequency channel. Frequency spectrum becomes broad after t=10s, when NB power increased suggesting change of turbulence characteristics. Figure 5 shows measured radial coherence. Clear difference was observed between low and high NB heating power. Radial correlation increased with increase of heating power and resultant increase of density peaking.

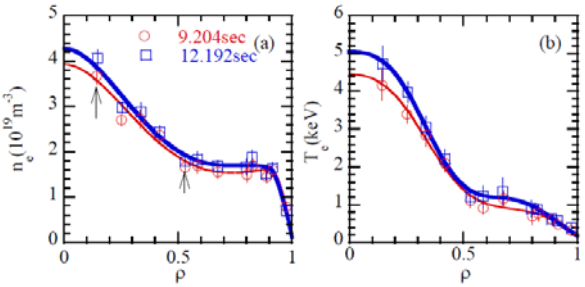

Fig.4 (a) n_e and (b) T_e profile at high (7.4MW, t=9.204s) and low (12.9MW, t=12.192s)NB power

The change of density scale length l_n=(1/n_e dn_e/dr)$^{-1}$ around cut off position of reflectmeter was estimated from two channel of YAG Thomson scattering, which were indicated by arrows in Fig. 4(a). Error bar of ln is due to the error of the measurements. As shown in Fig.3 (d), radial correlation length (l_c) increased with decrease of density scale length. Figure 6 shows relation between l_n and l_c and between l_n and cross power. The crossed power was estimated from the multi product between power spectrum and coherence spectrum and

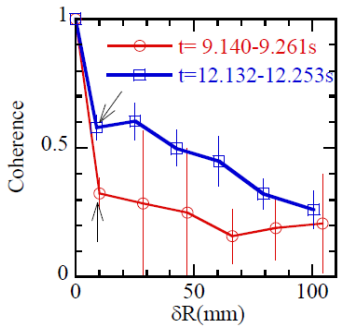

Fig.5 Radial coherence at ρ-0.3

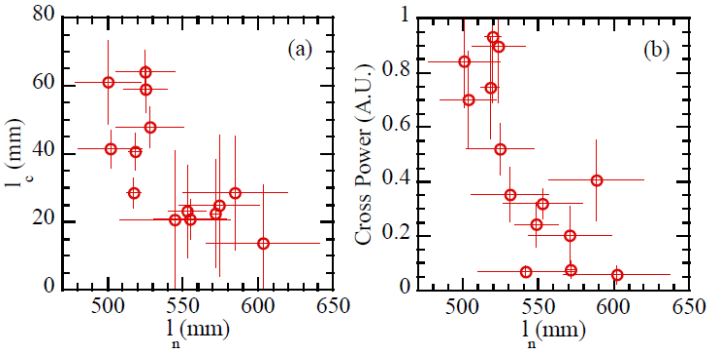

Fig.6 (a) Relation between ln and lc (b) Cross power and l_c

indicates power which has a radial spatial correlation. This was estimated from fixed frequency channel (47.3GHz) and closest channel (46.8GHz).

The reflected power would indicate fluctuation power at cut off position. Therefore, Figure 6 (a) and (b) shows that when density profile becomes peaked, fluctuation power increases and radial correlation becomes longer. The change of density profile in Fig.4 is not drastic, but this agrees the tendency shown in Fig.2, where density profile becomes peaked at lower collisionality. On the other hands, change of fluctuation power and radial correlation length is drastic. The density scale length is proportional to the V/D, where V is convection velocity and D is diffusion coefficient. Radial correlation length can indicate step size of radial diffusion. Thus, diffusion coefficient can be proportional to square of diffusion step. Therefore, Change of the radial correlation length from 20mm at low NB heating to 60mm at high NB heating suggests factor 9 difference of diffusion. This indicates inward convection increased factor 9 at least at high NB heating assuming constant l_n for the modest estimation.

The wavelength of the turbulence is around correlation length, thus, radial wavelength is around 20mm and 60mm for low and high NB heating cases. These correspond $k_{perp}\rho_s$=0.1-0.3 at cut off position, where k_{perp} is perpendicular wavenumber, where k_{perp} is perpendicular wavenumber is 0.16 and 0.05mm^{-1} for low and high heating power, and $\rho_s=c_s/\Omega_{ci}$, c_s and Ω_{ci} are ion sound speed and ion cyclotron frequency. This is slightly smaller than prediction of peak wavenumber of ITG/TEM from GS2 code, which is $k_{perp}\rho_s$=0.4-0.6 [6].

4. Response of turbulence under change of density profiles in LHD

Change of density profile under temporal scan of NB heating power is also observed in LHD. Figure 7 shows temporal behavior of density, temperature and fluctuation behavior. The fluctuation was measured by the two dimensional phase contrast imaging (2D-PCI). The measured wavenumber components are poloidally dominated [7]. As shown in Fig.7 (a) and (b), electron density decrease when NB power increases after t=4.1sec. This is opposite response to the one observed in JT-60U. However, it should be noted that there are two important differences between observations in JT-60U and LHD. One is magnetic configuration. As described in Sec.2, collisonality dependence of density peaking factor depends on magnetic configuration. The second difference is power deposition of NB heating. The particularity of NB heating in LHD described in this article is predominant electron heating, although NB heating in JT-60U in the data set of in this article is predominant ion heating. This is due to the high acceleration voltage (-160keV) of negative ion based neutral beam (N-NB). Especially, when density is low (line averaged density is less than -2x10^{19}m^{-3}), electron temperature is usually higher than ion temperature. As shown in Fig.7 (c), $T_e(0)/T_i(0)$

increases after t=4.1sec. In tokamak gyro-kinetic theory, increase of T_e/T_i can cause density flattening due to increase of thermo-diffusion, and fluctuation shifts from ITG to TEM [8]. This theoretical prediction qualitatively account for density flattening caused by electron cyclotron heating (ECRH) [9]. Density flattening observed in LHD is qualitatively similar to ECRH heating in tokamak.

As shown in Fig. 7 (d) and (e), fluctuation property changed with reduction of density. Measured wavenumber was poloidally dominated, thus, ploidal phase velocity in laboratory frame was measured by 2-D PCI. As shown in Fig 8 (d), phase velocity inside last closed flux surface was directed to the electron diamagnetic (e-dia.) direction before increase of NB power then switch to the ion diamagnetic (i-dia.) direction after increase of NB power. As shown in Fig. 8 (e), core (ρ=0.2-0.6) fluctuation power increased after increase of NB power.

Figure 9 shows radial profile of electric field (E_r), D, V, n_e, T_e profiles and fluctuation profiles at low (1MW, at t=4.0s) and high (5.6MW, at t=4.5s) NB power. The experimental values of D and V were estimated from density modulation experiments in this discharge. The radial electric fields were estimated from neoclassical am-bipolar condition. The neoclassical values (E_r, D and V) were estimated from GSRAKE code [9]. In Fig.9 (g), (h), (i), three different neoclassical values are shown art ρ>0.5. These are possible three roots of neoclassical am-bipolar condition.

As shown in Fig.8 (d) and (j), the n_e profiles changed from peaked one to flat one drastically. Especially reduction of density is very drastic at ρ < 0.6. The electron temperature increased around factor 1.5, however, temperature scale length, which is $l_t=(1/T_e\ dT_e/dr)^{-1}$, is almost constant. This is mainly due to the broad deposition of NB heating. It cannot be concluded from this data set if T_e profile is stiff like in tokamak. The change of density profiles is not due to the change of l_t but due to the change of T_e itself [10, 11]. The diffusion coefficients are anomaly large in whole region as shown in Fig.8 (b) and (h), although the difference of experimental D became closer to the neoclassical D at t=4.5s of high NB heating. The inward directed pinch was observed at t=4s of low NB heating and this becomes almost zero at t=4.5s of high NB heating, although neoclassical V indicates outward at both case. As described in Sec.II, neoclassical effect can play role on density profile at R_{ax}=3.6m, which is same configuration of data in Fig. 7 and 8. Especially convection velocity in core region ρ<0.7 is comparable with

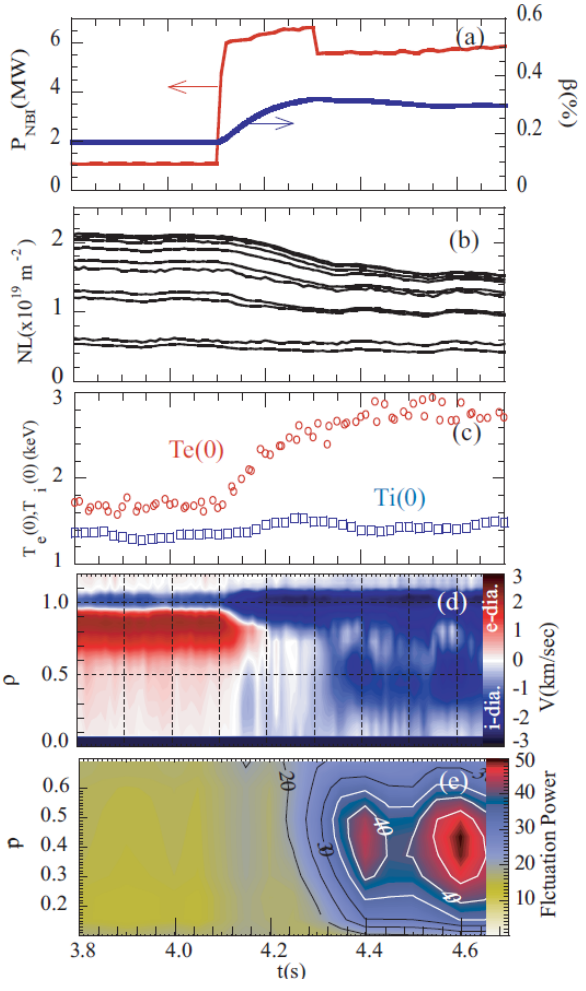

Fig.7 Time history of (a) NB heating power, diamagnetic β,(b) cnetral electron and ion temperature, (c) fluctuation phase velocity and (d) fluctuation power. In Fig.7(c), phase velocity propagatiing to electron diamag. R_{ax}=3.6m, Bt=2.75T.

neoclassical estimation and its T_e dependence is similar in experimental and neoclassical values at R_{ax}=3.6m [11]. However, still D is much larger than neoclassical values and direction of V does not agree with neoclassical estimation, therefore, the turbulence can play role on observed change of density profiles.

As shown in Fig.8 (e) and (k), strongest fluctuation power existed at around ρ=1.0. This is similar observations to toroidal devices. But another peaks were observed at around ρ=0.4 at both timing. The core fluctuation at around ρ=0.4 suggests to play role on change of density profiles, where string density reduction occurred. As shown in Fig.7 (d),(e) and Fig.8 (e), (k), fluctuation power in core region increased with increase of NB power, increase of T_e/T_i and decrease of density. In addition fluctuation phase velocity changed from e-dia. to i-dia. direction in laboratory frame. The neoclassical E_rxB_t rotation velocity was shown in Fig.8 (f) and (l). According to neoclassical estimation, poloidal rotation is directed to the e-dia. direction both at t=4.0 in ρ<1.0 and at t=4.5s in ρ<0.5. Thus change of observed phase velocity from e-dia. to i-dia. direction at ρ<0.5 can be due to change of phase velocity of fluctuation itself. Excluding E_rxB_t rotation, fluctuation phase velocity in plasma frame became almost zero at t=4.0s and switch to i-dia. direction at t=4.5s. Tokamak gyro-kinetic linear calculation shows switch from ITG to TEM with increase of T_e/T_i, but, in this case, poloidal phase velocity switches from i-dia, to e-dia. direction [9]. This does not agree with observations in LHD.

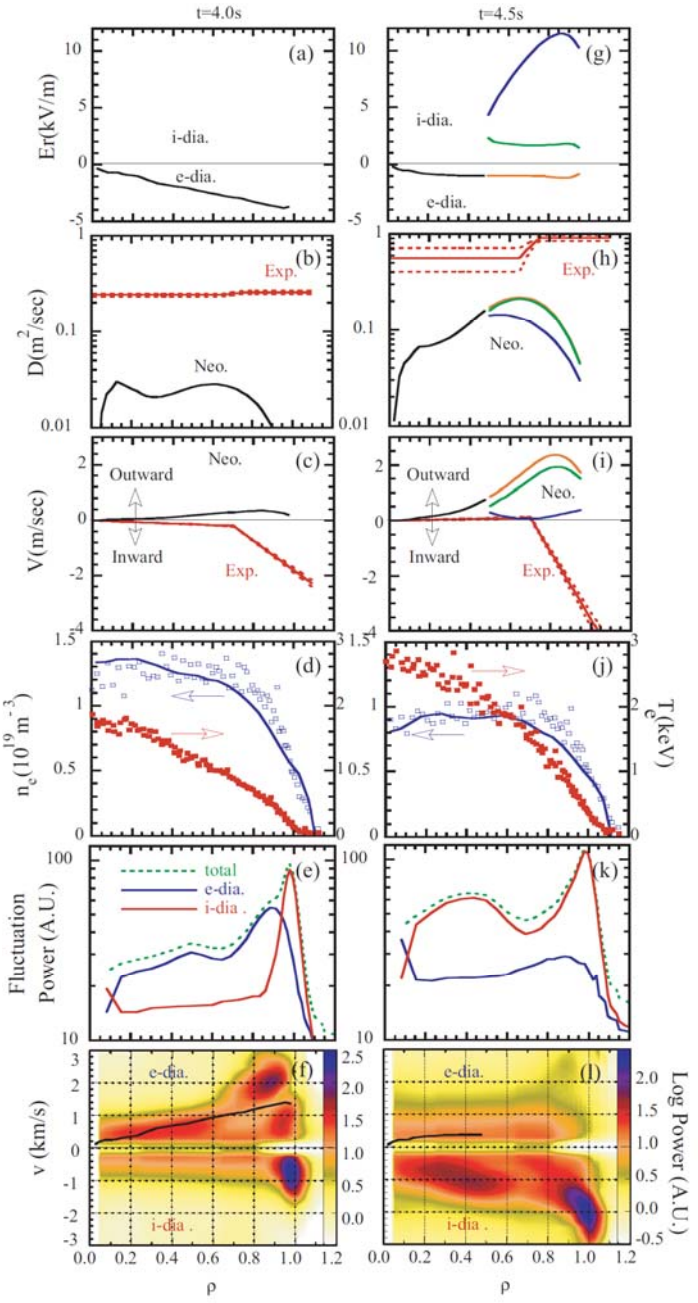

Fig.8 Radial profile of (a), (g) E_r, (b), (h) D, (c),(i) V,(d),(j) n_e T_e, (e), (k) fluctuation power and (f), (l) fluctaution phase velocity. (a)-(f) are at low NB power (1MW at t=4.0s) and (g)-(l) are at high NB power (5.6MW at t=4.5s). Neoclassical E_rxB_t roation velocities are indicated by black lines in Fig.8 (f) and (l).

The gyro-kinetic non linear simulation shows peak power at $k_{perp\_y}\rho_i$=0.1-0.3, where k_{perp_y} is poloidal wavenuber and ρ_i is ion Larmor radius[12]. At t=4.0s, experimental value of

$k_{perp\_y}\rho_i$ was 0.24 and 0.13 and at t=4 and 4.5 s respectively. These are within theoretical expectation.

5. Summary

In JT-60U and LHD, different collisionality dependence of density peaking factor was observed. In LHD, two different configurations (i.e. R_{ax}=3.5 and 3.6m) shows different collisionality dependence. Neoclassical contributions were comparable in both configuration, thus the difference was due to anomalous contribution. This was investigated in detail from density modulation experiments [11]. The change of the fluctuation character was observed in different density peaking at JT-60U with different NB power. At higher density peaking with higher NB power, fluctuation power became stronger and radial correlation became longer. Under modest change of density peaking, change of fluctuation property was drastic. In LHD, also change of fluctuation property was observed. With increase of NB power, core density reduced and fluctuation power increased and poloidal phase velocity changed from e-dia. to i-dia. direction in laboratory frame. The change of poloidal rotation should be checked by experimental measurements using charge exchange spectroscopy or heavy ion beam probe. The observed differences of density response can be partly due to the configuration difference between JT-60U and LHD and partly due to electron or ion heating. In both case, comparisons with linear/non-linear simulations are necessary for further understanding.

References

[1] TAKENAGA, H., et al., 2008 Nucl. Fusion **48** 075004
[2] TANAKA KA, K., et al., 2007 Fusion Sic. Tech **51** 97
[3] MURAKAMI, S., et al., 2002 Nucl. Fusion **42** L19
[4] ANGIONI, C., et al., 2003 Phys. Plasmas **10** 3225
[5] OYAMA, N., *in preparation*
[6] HILL, K.W., et al., 2002 Proc. 19th Int. Conf. on Fusion Energy 2002 (Lyon, 2002)
[7] TANAKA, K., et al., Rev. Sci. Instrum. in press
[8] ANGIONI, C., et al., 2004 Nucl. Fusion 44 827
[9] BEIDLER, C. D., et al., 1995 Plasma Phys. Control. Fusion, **37**, 463
[10] TANAKA, K., 2008 Nucl. Fusion 039801
[11] TANAKA, K., 2008 Plasma Fusion Res. 3, S1069
[12] WATANABE, T. H., et al., 2007 Nucl. Fusion **47** 1383